European Journal of Chemistry

Journal webpage: www.eurjchem.com

Some pyrazole derivatives as corrosion inhibitors for carbon steel in hydrochloric acid solutions

Mohamed Sobhi Motawea [1,2,*] and Mahmoud Ali Abdelaziz [2]

[1] *Department of Chemistry, Faculty of Science, Benha University, Benha, Qalubya, 13518, Egypt*
[2] *Department of Chemistry, Faculty of Science, University of Tabuk, Tabuk, 7149, Saudi Arabia*

** Corresponding author at: Department of Chemistry, Faculty of Science, University of Tabuk, Tabuk, 7149, Saudi Arabia. Tel.: +2.013.3269919. Fax: +2.013.3222578. E-mail address: mohamedsob7i@yahoo.com (M. Sobhi).*

ARTICLE INFORMATION

DOI: 10.5155/eurjchem.6.3.342-349.1279

Received: 07 June 2015
Accepted: 05 July 2015
Published online: 30 September 2015
Printed: 30 September 2015

KEYWORDS

Pyrazole
Steel surface
Carbon steel
Corrosion inhibitor
Langmuir isotherm
Pyrazole derivatives

ABSTRACT

Two pyrazole derivatives, namely 2,4-diamino-5-(5-amino-3-hydroxy-1*H*-pyrazole-1-carbonyl)thiophene-3-carbonitrile (I) and 1-(2,4-diamino-5-(5-amino-3-hydroxy-1*H*-pyrazole-1-carbonyl)thiophen-3-yl)propan-1-one (II) were evaluated as a corrosion inhibitors for carbon steel in 1M hydrochloric acid by weight loss, potentiodynamic polarization and electrochemical impedance spectroscopy methods. Spectrophotometric and conductometric titration methods were also utilized to investigate the possibilities of chemical adsorption between the steel surface and the compounds under consideration. The results showed that the studied compounds inhibit the corrosion of steel in acidic solution at different temperatures. The adsorption followed the Langmuir isotherm. The thermodynamic and the activation parameters were also determined and discussed.

Cite this: *Eur. J. Chem.* **2015**, *6(3)*, 342-349

1. Introduction

Acid solutions are used in industries in many processes such as pickling, acid cleaning and de-scaling of steel components [1]. The use of HCl in pickling of metals, acidization of oil wells and in the cleaning of scales is economically efficient and have low troubles compared to other known mineral acids. Because of the aggression effect of the most acid solutions, inhibitors of different kinds are commonly used to reduce the expected types of corrosion attack on metallic materials [2]. The protection using inhibitors is mainly based on the modification of the metal surface through the adsorption of inhibitor molecules and the subsequent formation of a protective blocking layer [3,4]. Most of the organic inhibitors adsorb on the metal surface by displacing water molecules on the surface and forming a compact barrier. The adsorption of an inhibitor mainly depends on the π-electrons and heteroatoms of the molecule which induces a great adsorption of the inhibitor molecules onto the steel surface. Most of the effective organic inhibitors contain heteroatoms such as O, N, S and multiple bonds in their molecules, which they can adsorb on the metal surface through them [5-10].

Much of the previous literatures reveal that heterocyclic compounds based on nitrogen such as the derivatives of pyrimidine, triazole, tetrazole, indole, pyridazine, benzimidazole [11-16] to mention but only few of these, have been used for the corrosion inhibition of iron or steel in acidic media. The effectiveness of pyrazole derivatives (*N*-heterocyclic compounds) as a corrosion inhibitors for carbon steel in hydrochloric acid media has been reported [17-19].The purpose of this study is to study the inhibiting action of the investigated pyrazole compounds on the corrosion behavior of carbon steel in 1 M HCl solution using various techniques.

2. Experimental

2.1. Materials

All the experiments were performed with carbon steel specimens of the following chemical composition (wt.%): 0.19% C, 0.05% Si, 0.94% Mn, 0.009% P, 0.004% S, 0.014% Ni, 0.009% Cr, 0.034% Al, 0.016% V, 0.003% Ti, 0.022% Cu, and balance Fe.

The investigated compounds used in this study were synthesized and characterized by Mohareb *et al.* [20] and shown in Figure 1.

ISSN 2153-2249 (Print) / ISSN 2153-2257 (Online)
http://dx.doi.org/10.5155/eurjchem.6.3.342-349.1279

Table 1. Corrosion parameters and the corresponding inhibition efficiencies for carbon steel in 1M HCl solution in the absence and presence of different concentrations of inhibitors at various temperatures obtained from weight loss measurements.

Temperature	Concentration	CR (mg cm^{-2} h^{-1}) of compounds		Θ of compounds		% IE of compounds	
(K)	(M)	I	II	I	II	I	II
303	Blank	2.93	2.93	-	-	-	-
	5×10^{-6}	0.70	0.61	0.76	0.79	76.10	79.20
	1×10^{-5}	0.61	0.50	0.79	0.82	79.10	82.90
	5×10^{-5}	0.53	0.43	0.82	0.85	82.00	85.35
	1×10^{-4}	0.31	0.24	0.89	0.91	89.40	91.80
	5×10^{-4}	0.24	0.18	0.92	0.93	92.00	93.80
313	Blank	5.03	5.03	-	-	-	-
	5×10^{-6}	1.11	1.00	0.77	0.80	77.90	80.11
	1×10^{-5}	1.03	0.84	0.79	0.83	79.60	83.30
	5×10^{-5}	0.87	0.68	0.82	0.86	82.70	86.50
	1×10^{-4}	0.50	0.42	0.90	0.91	90.00	91.70
	5×10^{-4}	0.37	0.33	0.92	0.93	92.70	93.40
323	Blank	8.60	8.60	-	-	-	-
	5×10^{-6}	1.69	1.51	0.80	0.82	80.30	82.50
	1×10^{-5}	1.45	1.33	0.83	0.84	83.10	84.60
	5×10^{-5}	1.33	1.17	0.84	0.86	84.60	86.40
	1×10^{-4}	0.66	0.56	0.92	0.93	92.30	93.50
	5×10^{-4}	0.48	0.42	0.94	0.95	94.40	95.00
333	Blank	15.00	15.00	-	-	-	-
	5×10^{-6}	2.96	2.84	0.80	0.81	80.30	81.00
	1×10^{-5}	2.54	2.33	0.83	0.84	83.00	84.40
	5×10^{-5}	2.31	2.06	0.84	0.86	84.60	86.30
	1×10^{-4}	1.17	1.05	0.92	0.93	92.20	93.50
	5×10^{-4}	0.81	0.73	0.94	0.95	94.60	95.00

The aggressive solution of 1 M HCl was prepared by dilution of analytical grade HCl (37%) with double distilled water and all experiments were carried out in unstirred solutions.

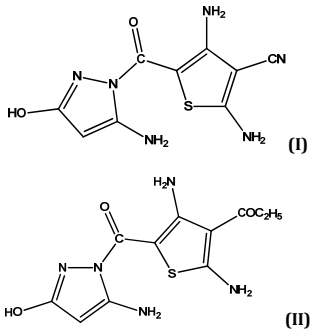

Figure 1. The chemical formula of compounds **I** and **II**.

2.2. Methods

Weight loss measurements were done using carbon steel sheets of 2.0×2.0×0.5 cm^3 which abraded with emery papers of grades 320, 600, 800 and 1200 then washed with bi-distilled water and acetone. After weighting accurately (using A&D HR-120 0.1 mg Analytical Balance), the specimens were immersed in a 250 mL beaker containing 250 mL 1.0 M HCl with and without the addition of different concentrations (5×10^{-6}, 1×10^{-5}, 5×10^{-5}, 1×10^{-4} and 5×10^{-4} M) of the investigated compounds. After an immersion time of 24 hours, the specimens were washed, dried, and weighted accurately. The same procedure was done at different temperatures varying from 303-333 K.

Potentiodynamic polarization measurements were performed using a carbon steel specimen in the form of a rod of 1 cm^2 exposed surface area as a working electrode. The measurements were carried out using Reference 600, GAMRY instruments potentiostate corrosion measurement system. Three compartment cell with saturated calomel reference electrode (SCE) and a platinum electrode was used as a counter electrode. Prior to polarization, the working electrode was abraded successively with emery paper (grades 320, 600, 800 and 1200) and washed thoroughly with de-ionized water, degreased with acetone and finally dried in a stream of air. The working electrode was introduced into the test solution and left for 30 min at the open circuit potential before starting the measurements at 5 mV/sec and 298 K.

Electrochemical impedance spectroscopy (EIS) measurements were performed a frequency range of 10-100 kHz and 5 mV signal amplitude perturbation using a computer-controlled potentiostate (Reference 600, GAMRY instruments).

The UV-visible spectrophotometric measurements were done by using JASCO UV-Vis 530 spectrophotometer and the conductance measurements were carried out using YSI model 32 conductance meter of cell constant equal to 1.6. The spectrophotometric and conductometric titration measurements were done as described previously [21].

3. Result and discussion

3.1. Weight loss measurements

3.1.1. Effect of inhibitor concentration

The values of corrosion rates (CR) and the percentage inhibition efficiency %IE calculated from weight loss measurements according to equations (1) and (2) [21] were listed in Table 1.

$$CR = \frac{\Delta m}{St} \quad (1)$$

$$\%\, IE = \frac{CR_{corr} - CR_{corr(inh)}}{CR_{corr}}\, x\, 100 \quad (2)$$

where Δm (mg), S (cm^2), t (h), CR_{corr} and $CR_{corr(inh)}$ represents the mass loss, surface area, immersion period and the corrosion rates in the absence and presence of inhibitors, respectively.

As shown from Table 1, the calculated values of corrosion rates, the inhibition efficiencies and the surface coverage were found to depend on the concentrations of the inhibitors. The corrosion rates (CR) decreased, whereas inhibition efficiencies %IE and the surface coverage values (θ) increased with increasing the inhibitor concentrations, reaching to maximum inhibition efficiency of %94.00 for compound **I** and %95.00 for compound **II** at 5×10^{-4} M after 24 hours of immersion. This may be attributed to the adsorption of the inhibitor molecules on the metal surface [21,22].

Table 2. Thermodynamic parameters of adsorption for carbon steel in 1 M HCl solution obtained from weight loss measurements.

Inhibitor system	Temperature (K)	K_{ads}×10^{-4}	ΔG^o_{ads}(kJ/mol)	ΔH^o_{ads}(kJ/mol)	ΔS^o_{ads}(J/mol.K)
Compound I	303	5.88	-37.78	26.18	211.08
	313	5.90	-39.03		208.33
	323	5.95	-40.30		205.82
	333	6.05	-41.60		203.54
Compound II	303	5.98	-37.82	26.95	213.76
	313	6.04	-39.09		211.00
	323	6.08	-40.36		208.39
	333	6.11	-41.63		205.94

The maximum decrease in the corrosion rate was observed for inhibitor **II**. The higher values of %IE given from inhibitor **II** may be attributed to an electron density rich of their functional groups in its constituents which may lead to easier bond formation, greater adsorption and consequently, higher inhibiting activity [23].

3.1.2. Effect of temperature on inhibition efficiency

The temperature effect on the corrosion rate and the %IE for carbon steel in 1 M HCl solution in the absence and in the presence of different concentrations of the investigated compounds was studied. From the given results in Table 1, one can see that the temperature increase from 303 to 333 K has no significant effect on the inhibition efficiency.

3.1.3. Adsorption isotherm

The values of surface coverage (θ) for different inhibitor concentrations in temperature ranges from 303 to 333 K were calculated according to the following equation;

$$\theta = \frac{W_o - W}{W_o} \quad (3)$$

where, W_o and W are the weight loss in the absence and in the presence of inhibitors, respectively, In the range temperature studied, the best correlation between the experimental results and the isotherm functions was obtained using Langmuir adsorption isotherm that given by;

$$\frac{C}{\theta} = \frac{1}{K_{ads}} + C \quad (4)$$

where, K_{ads} is the adsorptive equilibrium constant of the inhibitor adsorption process and C is the concentration of inhibitor.

Plots of C/θ against C for each temperature over the concentration range (5×10^{-6} -5×10^{-4} M) for compound **II** were drawn (Figure 2). Similar curves for compound **I** is not shown. The linear regression parameters are listed in Table 2. The results show that both the slopes and linear correlation coefficients are very close to one, indicating that the adsorption of the inhibitor molecules on the carbon steel surface in 1 M HCl solution obeys Langmuir isotherm [24]. K_{ads} values were calculated from the intercepts of the straight lines on the C/θ- axis and related to the standard free energy of adsorption, ΔG^o_{ads} according to the following equation;

$$\Delta G^o_{ads} = -RT \ln(55.5\, K_{ads}) \quad (5)$$

where, R is gas constant, T is temperature and 55.5 value is the molar concentration of water in solution in mol/dm^3. The adsorption heat, ΔH^o_{ads}, can be calculated by plotting ln K_{ads} and $1/T$ according to the Van't Hoff equation;

$$\ln K_{ads} = \left(\frac{-\Delta H^o_{ads}}{RT}\right) + const. \quad (6)$$

The standard entropy of adsorption ΔS^o_{ads} can be calculated from the thermodynamic basic equation as follows;

$$\Delta G^o_{ads} = \Delta H^o_{ads} - T\Delta S^o_{ads} \quad (7)$$

From the thermodynamic parameters listed in Table 2. It was observed that the values of ΔG^o_{ads}, being closer to -40 kJ/mol, is between the threshold values for physical adsorption and chemical adsorption indicating that adsorption of the inhibitor molecules on steel surface involves two types of interaction namely, adsorption and desorption processes [25]. The positive sign of the enthalpy ΔH^o_{ads} indicates an endothermic adsorption process. The positive sign of ΔS^o_{ads} indicates the substitution process, which can be attributed to the increase in the solvent entropy and more positive water desorption entropy [21].

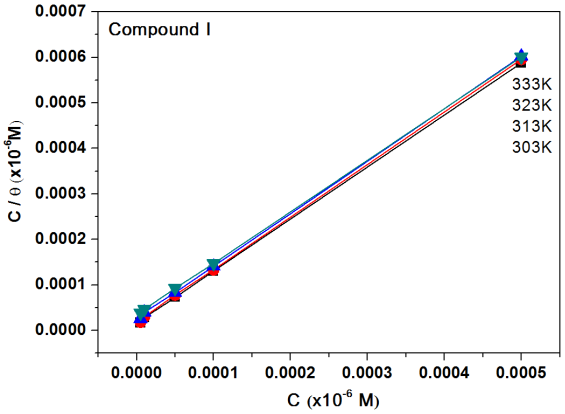

Figure 2. Langmuir isotherm adsorption model of the carbon steel surface of compound **II** in 1 M HCl solution at different temperatures.

3.1.4. Kinetic parameters

The kinetic model represents a useful tool for further explanation to the mechanism of corrosion inhibition. Figure 3 represents plot of the logarithm of the corrosion rate (mg/cm^2.h^{-1}) of carbon steel *vs.* 1000/T for carbon steel in 1 M HCl in absence and in the presence of compound **II** similar curves for compound **I** not shown. The activation energy (E_a) was evaluated by applying the equation below;

$$\ln CR = \frac{-E_a}{RT} + A \quad (8)$$

where, E_a is the apparent activation energy for carbon steel corrosion in 1 M HCl solution, R is the gas constant, A the Arrhenius pre-exponential factor and T is the absolute temperature. The values of E_a were calculated from the slope of the lines were given in Table 3. An alternative formula of the Arrhenius equation is the transition state equation:

$$CR = \frac{RT}{Nh} \exp\left(\frac{\Delta S^*}{R}\right) \exp\left(-\frac{\Delta H^*}{RT}\right) \quad (9)$$

where, h is the Planck's constant, N the Avogadro's number, ΔS^* the entropy of activation, and ΔH^* the enthalpy of activation.

Table 3. Activation parameters for the dissolution of carbon steel in 1 M HCl solution in the absence and presence of inhibitors.

Inhibitor system	Concentration (M)	E_a (kJ/mol)	ΔH^* (kJ/mol)	$-\Delta S^*$ (J/K.mol)
Blank	-	78.38	42.90	298.40
Compound I	5×10^{-6}	80.15	38.80	300.17
	1×10^{-5}	80.25	38.65	301.25
	5×10^{-5}	81.14	38.15	301.75
	1×10^{-4}	80.56	37.55	303.52
	5×10^{-4}	81.60	36.25	305.18
Compound II	5×10^{-6}	80.72	39.40	301.88
	1×10^{-5}	80.10	39.90	301.96
	5×10^{-5}	83.80	40.73	304.95
	1×10^{-4}	83.72	37.24	305.80
	5×10^{-4}	83.80	34.17	308.12

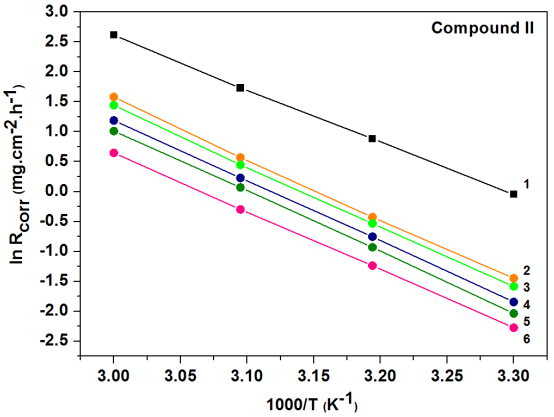

Figure 3. Arrhenius plots for carbon steel in 1 M HCl in the absence and presence of (1) 0.00 M, (2) 5×10^{-6} M, (3) 1×10^{-5} M, (4) 5×10^{-5} M, (5) 1×10^{-4} M, (6) 5×10^{-4} M of compound **II**.

A straight line relationship is obtained by plotting ln (CR/T) *vs.* 1000/T (Figure 4) with a slope of (-$\Delta H^*/R$) and an intercept of [(ln (R/Nh)) + ($\Delta S^*/R$)], from which the values of ΔS^* and ΔH^* were calculated. From of the data listed in Table 3. It is clear that the values of E_a determined in the presence of the inhibitor molecules are higher than that in the absence of inhibitors (blank). The increase in E_a in the presence of inhibitor indicates the physical adsorption that occurs in the first stage [23]. The positive sign of the enthalpies ΔH^* reflects the endothermic nature of the steel dissolution process and that mean the dissolution of steel is difficult. Values of ΔS^* for the inhibited solution were higher than those for the uninhibited one and suggests the increase in randomness occurred on going from reactants to the activated complex.

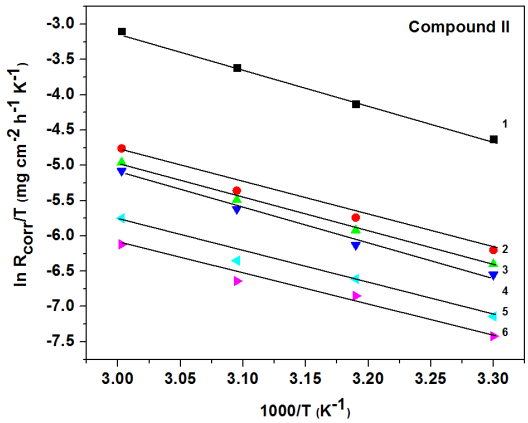

Figure 4. Plot of ln (CR/T) *vs.* 1000/T for carbon steel in 1 M HCl in the absence and presence of (1) 0.00 M, (2) 5×10^{-6} M, (3) 1×10^{-5} M, (4) 5×10^{-5} M, (5) 1×10^{-4} M, (6) 5×10^{-4} M of compound **II**.

3.2. Potentiodynamic polarization measurements

Figure 5 shows the carbon steel polarization curves in absence and in the presence of different concentrations of compound **II** at 303 K, similar curves for compound **I** is not shown. Table 4, show the electrochemical corrosion parameters, i.e., corrosion potential (E_{corr}), cathodic and anodic Tafel slopes (β_c, β_a) and corrosion current density I_{corr} obtained by extrapolating the Tafel anodic and cathodic linear parts until they intersect [21]. The inhibition efficiency was calculated by using the following equation;

$$\%\, IE_{(a)} = \left[1 - \frac{I_{corr}}{I^o_{corr}}\right] x100 \qquad (10)$$

where, I_{corr} and I^o_{corr} are the corrosion current densities in the absence and in the presence of inhibitors, respectively.

As it can be seen from Figure 5, the current density of both cathodic and anodic branches is shifted towards lower values which are more evident with increasing the inhibitor concentration compared to the blank. Also, the values of the corrosion potential (E_{corr}) does not remarkably shift in the presence of the inhibitors, therefore, the tested inhibitors can be identified as mixed anodic and cathodic inhibitor [24].

The values of cathodic Tafel slopes (β_c) increases by increasing the inhibitor concentration, indicating that the inhibitor molecules are firstly adsorbed onto steel surface and then impedes by merely blocking the active sites of the steel surface. In a similar manner, β_a shows higher values in the inhibited solutions than that obtained for the blank. The increase in β_a suggesting that the inhibition mechanism involves an interposition of the inhibitor molecules into the anodic charge transfer process, leading to some type morphological change of the electrode brought about by the anodic dissolution [22]. According to $\%IE_{(a)}$ values shown in Table 4, the inhibiting properties of the investigated inhibitors can be given in the following order: **II** > **I**, which is in a good agreement with that calculated from weight loss technique.

3.3. Electrochemical impedance spectroscopy studies

Nyquist plot for carbon steel in 1 M HCl solution in the absence and in the presence of different concentrations of inhibitor at 298 K was given in Figure 6. The obtained spectra shows a single semicircle and the diameter increases with increasing the concentration of the inhbitor. This diagram exhibit that the impedance spectra consist of one capacitive loop at high frequency, the high frequency capacitive loop was attributed to charge transfer of the corrosion process [26]. To determine the impedance parameters, Table 4, the measured impedance data were analyzed, based on the electric equivalent circuit presented in our previous study [24]. This circuit consists of R_s (the resistance of solution between the carbon steel electrode surface and the counter electrode), the double-layer capacitance (C_{dl}) in parallel to the charge-transfer resistance (R_{ct}).

Table 4. The electrochemical and corrosion parameters carbon steel in the absence and presence of different concentrations of inhibitors in 1M HCl solution at 30 °C calculated from both potentiodynamic polarization and EIS measurements.

Inhibitor system	Conc. (M)	$E_{corr.}$ (mV, SCE)	β_a (mV/dec)	β_c (mV/dec)	I_{corr} (mA/cm²)	%I.E [a]	R_s (Ω cm²)	R_{ct} (Ω cm²)	C_{dl} (μF/cm²)	%I.E [b]
Blank	HCl (1M)	-425	174	-134	0.411	-	1.95	51	109	-
Compound I	5×10^{-6}	-443	238	-151	0.0832	79.75	1.70	286	36.12	82.20
	1×10^{-5}	-441	211	-153	0.0760	82.00	1.65	343	23.50	85.15
	5×10^{-5}	-448	217	-173	0.0622	84.90	1.82	516	19.15	90.15
	1×10^{-4}	-445	221	-168	0.0335	91.85	1.75	570	11.50	91.00
	5×10^{-4}	-446	203	-175	0.0288	93.00	1.90	736	8.00	93.00
Compound II	5×10^{-6}	-451	246	-158	0.081	80.30	1.84	328	31.50	84.45
	1×10^{-5}	-448	251	-161	0.070	83.00	1.76	403	21.20	87.30
	5×10^{-5}	-453	243	-166	0.056	86.40	1.75	576	14.50	91.10
	1×10^{-4}	-455	253	-170	0.029	92.90	1.90	656	10.18	92.30
	5×10^{-4}	-456	258	-181	0.021	94.90	1.85	783	6.80	93.50

[a] Inhibition efficiency calculated from polarization measurements.
[b] Inhibition efficiency calculated from EIS measurements.

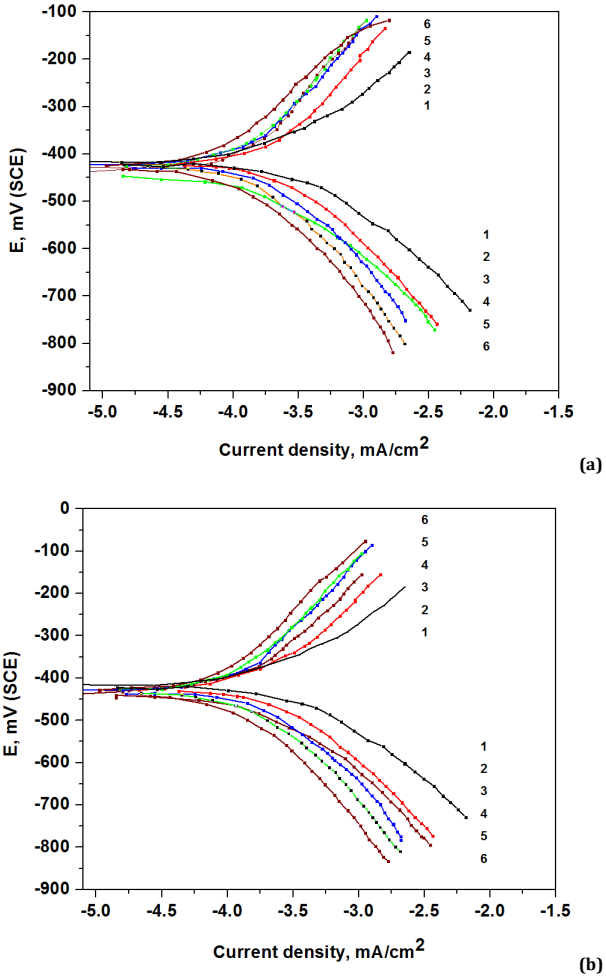

Figure 5. Potentiodynamic polarization curves of carbon steel in 1 M HCl solution in the absence and presence of different concentrations of (a) compound **I**: (1) blank, (2) 5.0×10^{-6}, (3) 1.0×10^{-5}, (4) 5.0×10^{-5}, (5) 1.0×10^{-4}, (6) 5.0×10^{-4} M. (b) Compound **II**: (1) blank, (2) 5.0×10^{-6}, (3) 1.0×10^{-5}, (4) 5.0×10^{-5}, (5) 1.0×10^{-4}, (6) 5.0×10^{-4} M.

The values of R_{ct} were calculated from the difference in impedance at lower and higher frequencies as suggested by Tsuru *et al.* [27]. C_{dl} values were calculated from the frequency at which the imaginary component of impedance was maximum (Z_i max) using the relation [28];

$$C_{dl} = \frac{1}{2\pi f_{max}} \frac{1}{R_{ct}} \quad (11)$$

where, f_{max} is the frequency at which the imaginary component of impedance is maximum. The inhibition efficiency got from the charge-transfer resistance is calculated by the following relation [21]:

$$\%IE_{(b)} = \left[\frac{(1/R_{ct})_o - (1/R_{ct})}{(1/R_{ct})_o}\right] x100 \quad (12)$$

where, $(R_{ct})_o$ and (R_{ct}) are the charge transfer resistance densities in the absence and in the presence of inhibitors, respectively.

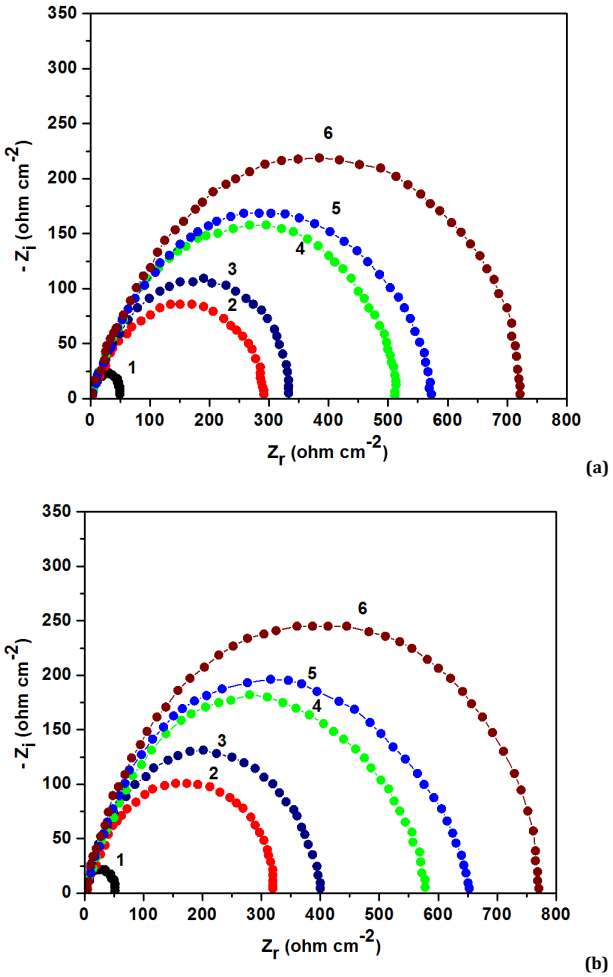

Figure 6. Nyquist plots for carbon steel in 1 M HCl in the absence and presence of different concentrations of (a) compound **I**: (1) blank, (1) 5.0×10^{-6}, (2) 1.0×10^{-5}, (3) 5.0×10^{-5}, (4) 1.0×10^{-4}, (5) 5.0×10^{-4} M (b) Compound **II**: (1) blank, (1) 5.0×10^{-6}, (2) 1.0×10^{-5}, (3) 5.0×10^{-5}, (4) 1.0×10^{-4}, (5) 5.0×10^{-4} M.

As can be seen from Table 4, the R_{ct} values of the investigated compounds increase with increasing inhibitor concentration. At the same time the C_{dl} has the opposite trend in the whole concentration range. This behavior could be due to a decrease in dielectric and/or an increase in the thickness of the electrical double layer, resulting from the gradual replacement of water molecules and other ions originally adsorbed on the surface by adsorption of inhibitor molecules on metal-solution interface, resulting in a barrier film formation on the carbon steel surface, and hence decreasing the rate of anodic dissolution processes [29].

3.4. UV-visible spectra

The formation of the investigated inhibitor complexes with iron ions released during the corrosion reaction was studied by means of UV-Vis spectroscopy. Figure 7 shows the electronic absorption spectra of the free iron ions, compound **II**, and the produced compound **II**-iron complex, respectively. Figure 7 shows band at λ_{max} = 285 nm which can be ascribed to π-π* transition of the benzenoid system of the inhibitor molecule, and another bands at λ_{max} = 390 nm which can be attributed to n-π* transitions within the heterocyclic moiety of the compound. Interestingly, this bands that are due to n-π* transition heterocyclic moiety disappeared upon complexation, as clear in Figure 7, suggesting the interaction between inhibitor molecules and Fe^{+2} ions in the solution to form Fe^{+2}-Inhibitor complex. It is noteworthy that these experimental findings give a good evidence for the possible formation of a complex between Fe^{+2} cation and the inhibitor molecules in 1 M HCl.

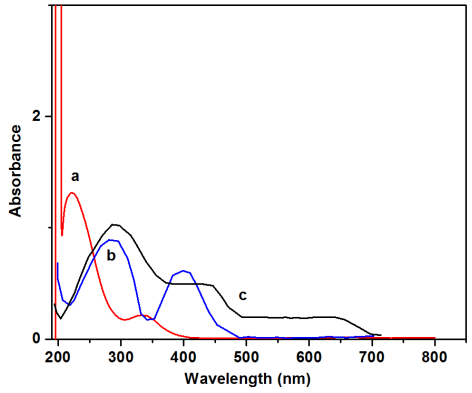

Figure 7. UV absorption spectra of: (a) Fe^{+2}, (b) inhibitor (II) and (c) Fe^{+2} - inhibitor complex, the concentrations of Fe^{+2} and inhibitor were 1×10^{-3} M.

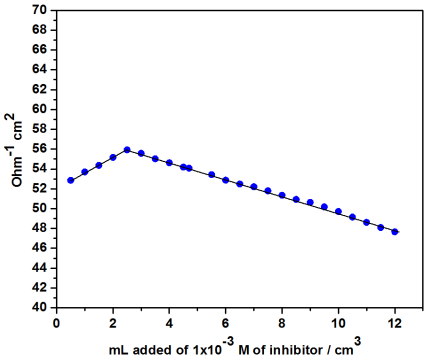

Figure 8. Conductometric titration curve for 50 cm^3 1×10^{-4} M Fe^{+2} cation titrated with different volumes of 1×10^{-3} M of inhibitor **II** solution.

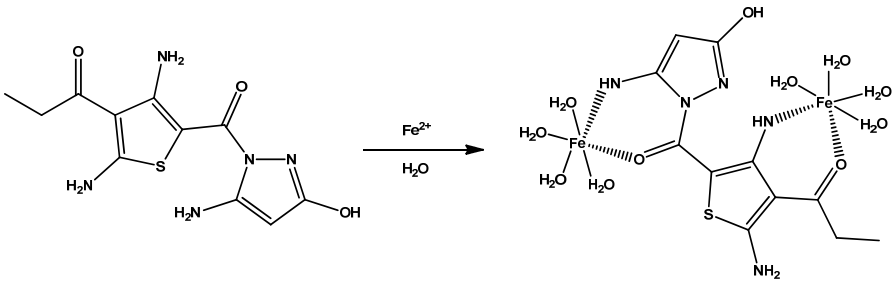

Figure 9. Chemical formula of compound **II -** Fe $^{+2}$ complex.

3.5. Conductometric measurements

The plot of the specific conductance values obtained for Fe^{+2} cation, after correction for the dilution effect, *vs*., mL added of 1×10^{-3} M of compound **II** is shown in Figure 8. It is known that conductance values depend on some factors such as volume, concentration of ionic species, *etc*. In our case, this depends to a large extent on the reaction taking place between the ligand and metal ions in solution. The ions liable to exist in solution are the H$^+$ ions which are produced by displacement from the ligand molecule by metal ions. Thus, complex formation should take place through a covalent link construction between the metal ion and the oxygen atom of the amine group [30]. Hence, it can be concluded that the conductance of the titrated solution is mainly due to Fe^{+2} cation. After the complex formation of 2:1 (Fe^{+2}: Inhibitor) complex type, the conductance values tends to decrease which may be attributed to the increase in the volume of the species (i.e. complex) and in turn the mobility of the complex becomes less than that of the ions present in the solution on increasing the amount of titrant at 25 °C [31], as shown in Figure 8. Consequently, it can be concluded that the complex formed may be have the proposed structure in Figure 9.

3.6. Inhibition mechanism

As investigated from the above results, the adsorption of the investigated inhibitor molecules on steel surface can not be considered as purely physical or purely chemical adsorption phenomenon. As shown from the calculated thermodynamic parameters given in Table 2, the adsorption of the inhibitor molecules on the carbon steel surface in 1.0 M HCl solution is more chemical adsorption than physical adsorption. The chemical type of adsorption may arises from the presence of donor-acceptor interactions between free electron pairs of hetero atoms and π-electrons of multiple bonds as well as phenyl group within the inhibitor molecules and vacant *d* orbitals of iron [21]. In addition to the chemical adsorption, the inhibitor molecules can also be adsorbed on the steel surface via electrostatic interaction between the charged metal surface and the charged inhibitor molecules formed within the medium through electrostatic interactions between the negatively charged metal surface and positively charged inhibitor molecules to form a protective $(FeCl^- \text{ Inhibitor}^+)_{ads}$ layer [21].

4. Conclusions

From the above collected results, the following conclusions may be drawn easily:

1. The investigated compounds inhibit the corrosion of carbon steel hydrochloric acid solution and their %IE increases with increasing their concentration in the range of temperature studied.
2. The adsorption of the inhibitors on steel surface is found to obey the Langmuir adsorption isotherm.
3. The potentiodynamic polarization data indicated that the investigated inhibitors are of mixed type.
4. EIS measurements revealed that the R_{ct} decrease with respect to the blank solution by addition of inhibitor.
5. The UV-visible and conductometric titration measurements reveal the formation of Fe-inhibitor complex, which may be responsible for the observed inhibition.

References

[1]. Mohan, P.; Kalaignan, G.P. *J. Mater. Sci. Technol.* **2013**, *29*, 1096-1100.
[2]. Li, X.; Deng, S.; Fu, H.; Li, T. *Electrochim. Acta* **2009**, *54*, 4089-4098.
[3]. Abdallah, M.; Meghed, H.E.; Sobhi, M. *Mater. Chem. Phys.* **2009**, *118*, 111-117.
[4]. Abdallah, M.; Meghed, H.E.; Sobhi, M. *Monats. Chem*. **2010**, *141*, 1287-1298.

[5]. Amin, M. A.; Ibrahim, M. M. *Corros. Sci.* **2011**, *53*, 873-885.
[6]. Aouniti, A.; Hammouti, B.; Brighli, M.; Kertit, S.; Berhili, F.; ElKadiri, S.; Ramdani, A. *J. Chim. Phys.* **1996**, *93*, 1262-1271.
[7]. Abdallah, M.; El-Naggar, M. M. *Mater. Chem. Phys.* **2001**, *71*, 291-298.
[8]. Gad Allah, A. G.; Tamous, H. M. *J. Appl. Electrochem*. **1990**, *20*, 488-493.
[9]. Gad Allah, A. G.; Moustafa, H. *J. Appl. Electrochem*. **1992**, *22*, 644-648.
[10]. Khaled, K. F.; Amin, M. A. *Corros. Sci*. **2009**, *51(90)*, 1964-1975.
[11]. Abd El-Maksoud, S. A. *Appl. Surf. Sci*. **2003**, *206*, 129-136.
[12]. Hassan, H. H.; Abdelghani, E.; Amina, M. A. *Electrochim. Acta* **2007**, *52*, 6359-6366.
[13]. Kertit, S.; Hammouti, B. *Appl. Surf. Sci*. **1996**, *61*, 59-66.
[14]. Khaled, K. F. Mater. *Chem. Phys*. **2008**, *112*, 290-300.
[15]. Chetouani, A.; Aounti, A.; Hammouti, B.; Benchat, N.; Benhadda, T.; Kertit, S. *Corros. Sci*. **2003**, *45*, 1675-1684.
[16]. Wahdan, M. H. *Mater. Chem. Phys.* **1997**, *49*, 135-140.
[17]. Mahendra, Y.; Rajesh, R. S.; Tarun, K. S.; Nidhi, T. *J. Adhes. Sci. Technol.* **2015**, *29(16)*, 1690-1713.
[18]. Chetouani, A.; Hammouti, B.; Benhadda, T.; Daoudi, M. *Appl. Surf. Sci*. **2005**, *249*, 375-385.
[19]. Abdel-Rehim, S. S.; Khaled, K. F.; Al-Mobarak, N. A. *Arap. J. Chem.* **2011**, *4(3)*, 333-337.
[20]. Mohareb, R. M.; El-Sayed, N. N.; Abdelaziz, M. A. *Molecules* **2012**, *17*, 8449-8463.
[21]. Sobhi, M. *Prot. Met. Phys. Chem*. **2014**, *50(6)*, 825-832.
[22]. Sobhi, M.; Abdallah, El-Sayed, R. *J. Surf. Deterg*. **2013**, *16*, 937-946.
[23]. Larabi, L.; Harek, Y.; Benali, O.; Ghalem, S. *Prog. Org. Coat.* **2005**, *54*, 256-262.
[24]. Sobhi, M.; Abdallah, M.; Khairou, K. S. *Monatsh. Chem*. **2012**, *143*, 1379-1387.
[25]. Yart, A.; Ultras, S.; Dal, H. *Appl. Surf. Sci*. **2006**, *253*, 919-925.
[26]. Ashassi-Sorkhabi, H.; Ghatebsaz-Jeddi, N.; Hashemzadeh, F.; Jahani, H. *Electrochim. Acta* **2006**, *51*, 3848-3854.
[27]. Tsuru, T.; Haruyama, S.; Gijutu, B. J. *Japan. Soc. Corros. Eng*. **1978**, *27*, 573-579.
[28]. Zhang, S.; Tao, Z.; Li, W.; Hou, B. *Appl. Surf. Sci*. **2009**, *255*, 6757-6763.
[29]. Lagrenee, M.; Mernari, B.; Bouanis, M.; Traisnel, M. *Corros. Sci.* **2002**, *44*, 573-588.
[30]. Amin, A. S. *Analysis* **1995**, *23*, 415-417.
[31]. Kottaf, I. M.; Elving, P. I. Treatise on analytical chemistry (Part I), Interscience, New York, 1963.